

RESEARCH

Open Access



Recognition of warheads by range-profile matching with automatic threshold

Donglin Tan^{1*}  and Junfeng Wang¹

*Correspondence:
johnnytan@sjtu.edu.cn

¹ Department of Electronic
Engineering, Shanghai Jiao Tong
University, Shanghai, China

Abstract

In this paper, a novel algorithm is presented for warhead recognition in the defense of ballistic missiles. The range profiles from the warheads of interest in typical illumination directions form a dataset. First, each range profile in the dataset is compared to the range profile of the target under observation, and the most similar range profile is found. Then, the observed target is considered as a warhead if the deviation of its range profile from the most similar range profile is less than or equal to a threshold. The threshold is chosen such that the detection rate is a constant. The simulation results verify the effectiveness of the proposed algorithm. Since the threshold is automatically calculated according to the detection rate, this algorithm has a larger applicability than the current methods based on range-profile matching.

Keywords: Radar signal processing, Radar target recognition, Range-profile matching, Recognition threshold

1 Introduction

With the development of ballistic missile technology, the threat of ballistic missiles becomes more and more severe in modern wars, and the defense of ballistic missiles is therefore getting more and more important. Ballistic missile defense requires a warning time as long as possible, accurate trajectory computation, accurate intercept control, and timely effect assessment. However, according to a penetration technology, ballistic missile may release not only warheads, but also decoys in its midcourse, which makes its defense become very difficult [1–5]. The effective recognition of warheads from decoys thus has to be handled in the defense of ballistic missiles and has become a most challenging problem in ballistic missile defense systems.

The features in radar cross section (RCS), shape, micro-motion, etc., can be used to recognize warheads from decoys. Simple decoys, like spheres and fragments, may be excluded according to their features in RCS [6] and shape. High-imitation decoys may be excluded according to their micro-motion features because high-imitation decoys have different masses and mass distributions and thus different micro-motion features from warheads [7–9].

The features of a target can be extracted from its echo energy, range profile, inverse synthetic aperture radar (ISAR) image or interferometric ISAR (InISAR) image. Since it cannot

reflect the shape features of the target, the echo energy is unfit for warhead recognition. ISAR can generate the two-dimensional image of the target. It uses a wideband technique to achieve fine range resolution and utilizes the rotation of the target relative to the radar boresight to achieve fine azimuth resolution. Furthermore, InISAR can generate the three-dimensional image of the target, where the third-dimension information is extracted from the interferometric phase of the ISAR images from different channels [10]. Theoretically, an ISAR or InISAR image can describe the shape features of the target. However, it also has quite a few limitations in warhead recognition [11]. On one hand, the imaging algorithms are not reliable enough. On the other hand, even if the imaging algorithms are perfect, the imaging of the target still requires rotation of the target relative to the radar boresight. In contrast, with the widespread application of wideband radars, the range profile is becoming a feasible and reliable option for warhead recognition [12–14]. The range profile can be obtained accurately in real time and reflect the projection of the target in range [15, 16].

The range-profile matching is a simple but effective method for warhead recognition. A target is regarded as a warhead if the similarity of its range profile to the one of a warhead is larger than a threshold. There are many methods to measure the similarity between two range profiles, such as correlation coefficient, exponent coefficient [17, 18]. However, traditionally, the threshold is chosen empirically [19] and has to be chosen again if the observation condition changes.

In this paper, we present an algorithm for warhead recognition by the range-profile matching. The range profiles from the warheads of interest in typical illumination directions form a dataset. Each range profile in the dataset is compared to the range profile of the target under observation, and the most similar range profile is found. The target is considered as a warhead if the deviation of its range profile from the most similar range profile is less than or equal to a threshold. For warhead recognition, the probability distribution of the deviation is unpredictable for decoys but stable for warheads, and therefore, the threshold is chosen such that the detection rate is a constant. Since the threshold is automatically calculated according to the detection rate, this algorithm has a larger applicability than the current methods based on range-profile matching. Preliminary results of this work have been given in [20].

2 Range-profile matching

In order to recognize warheads by the range-profile matching, a dataset needs to be set up. Depending the implementation conditions, this dataset can be set up by field experiments, experiments in anechoic chambers or computer simulation. This dataset consists of the range profiles from the warheads of interest in typical illumination directions. In the proposed algorithm, first, each range profile in the dataset is compared to the range profile of the target under observation, and the most similar range profile is found.

The normalized maximum correlation is used to measure the similarity between two range profiles. Assume that $x(n)$ is the range profile of the target, and $s_k(n)$ is the k -th range profile in the dataset. The correlation function of $x(n)$ with $s_k(n)$ is defined as

$$r_k(m) = \sum_{n=-\infty}^{\infty} x(n)s_k(n-m), \quad (1)$$

where m is the shift of $s_k(n)$. The normalized maximum correlation of $x(n)$ with $s_k(n)$ is defined as

$$R_k = \frac{\max_m [r_k(m)]}{\sqrt{\sum_{n=-\infty}^{\infty} x^2(n)} \sqrt{\sum_{n=-\infty}^{\infty} s_k^2(n)}}. \tag{2}$$

Evidently, R_k can be used to measure the similarity between $x(n)$ and $s_k(n)$.

The range profile with the largest R_k among all the range profiles in the dataset is the most similar to the range profile of the target. It will be used to determine whether the target is a warhead.

3 Recognition based on deviation

The target is regarded as a warhead if the deviation of its range profile from the most similar range profile in the dataset is less than or equal to a threshold. The definition and the threshold of the deviation will be given in this section. For a radar recognition system, the false alarm rate is also an important parameter that must be discussed. The false alarm rate here is defined as the probability that a non-warhead target is misjudged as a warhead. And the calculation derivation of the false alarm rate will also be given in this section.

3.1 Definition of deviation

Assume that $x(n)$ is the range profile of the target, and $s(n)$ is the most similar range profile in the dataset. Here, $s(n)$ has been shifted such that its correlation function with $x(n)$ is maximized. Moreover, $x(n)$ and $s(n)$ are limited to a proper interval $1 \leq n \leq N$. The deviation of $x(n)$ from $s(n)$ is defined as

$$D = \sqrt{\sum_{n=1}^N d_n^2}, \tag{3}$$

where d_n is the difference between the normalized range profile of the target and the normalized range profile in the dataset:

$$d_n = \frac{x(n)}{\sqrt{\sum_{n=1}^N x^2(n)}} - \frac{s(n)}{\sqrt{\sum_{n=1}^N s^2(n)}}. \tag{4}$$

Actually, the deviation is the norm of the difference between the unitized $x(n)$ and the unitized $s(n)$.

D can be written as

$$D = \sqrt{2 - 2R}, \tag{5}$$

where R is the normalized correlation of $x(n)$ with $s(n)$, i.e.,

$$R = \frac{\sum_{n=1}^N [x(n)s(n)]}{\sqrt{\sum_{n=1}^N x^2(n)} \sqrt{\sum_{n=1}^N s^2(n)}}. \tag{6}$$

Equation (5) implies that D and R are equivalent in determining whether the target is a warhead. The target can be regarded as a warhead if R is larger than or equal to a corresponding threshold. Equivalently, the target can be regarded as a warhead if D is less than or equal to a threshold. Nonetheless, it is significant to introduce D because a method can thus be developed to choose the threshold automatically, as will be shown next.

3.2 Threshold of deviation

For warhead recognition, since the probability distribution of the deviation is unpredictable for decoys but stable for warheads, the threshold can be chosen such that the detection rate is a constant. We call this method the constant detection rate (CDR) method, in contrast with the constant false alarm rate (CFAR) method [21] in the detection theory.

Let $x_\mu(n)$, $x_v(n)$, $s_\mu(n)$ and $s_v(n)$ be the signal in $x(n)$, the noise in $x(n)$, the signal in $s(n)$ and the noise in $s(n)$, respectively. It should be noted that if the dataset is set up by computer simulation, $s_v(n)$ can be set as 0. However, in practice, there is unavoidable noise in $s(n)$, and thus, $s_v(n)$ is not 0. If the signal-to-noise ratios (SNRs) of $x(n)$ and $s(n)$ are high enough, Eq. (4) can be written as

$$d_n = \frac{x_\mu(n) + x_v(n)}{\sqrt{\sum_{n=1}^N x_\mu^2(n)}} - \frac{s_\mu(n) + s_v(n)}{\sqrt{\sum_{n=1}^N s_\mu^2(n)}}. \tag{7}$$

In this article, the SNR is defined as the ratio of the total energy of the signal to the total energy of the noise. Let $x(n)$ be a range profile of a warhead and $s(n)$ be its corresponding range profile in the dataset. Then, since the signals are canceled, i.e.,

$$\frac{x_\mu(n)}{\sqrt{\sum_{n=1}^N x_\mu^2(n)}} = \frac{s_\mu(n)}{\sqrt{\sum_{n=1}^N s_\mu^2(n)}}, \tag{8}$$

Equation (7) can be written as

$$d_n = \frac{x_v(n)}{\sqrt{\sum_{n=1}^N x_\mu^2(n)}} - \frac{s_v(n)}{\sqrt{\sum_{n=1}^N s_\mu^2(n)}}. \tag{9}$$

The standard deviation of d_n is

$$\sigma = \sqrt{\frac{\text{var}[x_v(n)]}{\sum_{n=1}^N x_\mu^2(n)} + \frac{\text{var}[s_v(n)]}{\sum_{n=1}^N s_\mu^2(n)} - \frac{2\text{cov}[x_v(n), s_v(n)]}{\sqrt{\sum_{n=1}^N x_\mu^2(n)}\sqrt{\sum_{n=1}^N s_\mu^2(n)}}}. \tag{10}$$

$x_v(n)$ and $s_v(n)$ are independent generally, and thus, Eq. (10) can be written as

$$\sigma = \sqrt{\frac{\text{var}[x_v(n)]}{\sum_{n=1}^N x_\mu^2(n)} + \frac{\text{var}[s_v(n)]}{\sum_{n=1}^N s_\mu^2(n)}}. \tag{11}$$

Assume that $x_v(n)$ and $s_v(n)$ are 0-mean. Then, d_n is also 0-mean. In addition, Eq. (11) can be written as

$$\sigma = \sqrt{\frac{1}{N} \left(\frac{1}{\text{SNR}_x} + \frac{1}{\text{SNR}_s} \right)}, \tag{12}$$

where SNR_x and SNR_s are the SNRs of $x(n)$ and $s(n)$, respectively. Further, assume that d_1, d_2, \dots, d_N are independent Gaussian random variables. Then, the probability density function of d_1, d_2, \dots, d_N is [22]

$$f(d_1, d_2, \dots, d_N) = \frac{1}{(\sqrt{2\pi}\sigma)^N} \exp\left(-\frac{1}{2\sigma^2} \sum_{n=1}^N d_n^2\right). \tag{13}$$

Let T be the threshold. Then, the detection rate (the probability that the warhead is regarded as a warhead) is the probability that the deviation of the warhead is less than or equal to T . According to Eq. (13), the detection rate can be written as

$$P_d = \int_{\Omega} \frac{1}{(\sqrt{2\pi}\sigma)^N} \exp\left(-\frac{1}{2\sigma^2} \sum_{n=1}^N d_n^2\right) dv, \tag{14}$$

where Ω is a hypersphere given by

$$\sqrt{\sum_{n=1}^N d_n^2} \leq T. \tag{15}$$

By choosing the probability between the hyper spherical surface with the radius r and the hyper spherical surface with the radius $r + dr$ as the integral element, Eq. (14) is converted into

$$P_d = \int_0^T \frac{1}{(\sqrt{2\pi}\sigma)^N} \exp\left(-\frac{r^2}{2\sigma^2}\right) S_N(r) dr. \tag{16}$$

where $S_N(r)$ is the area of the N -dimensional hyper spherical surface with the radius r . According to [23], $S_N(r)$ is given by

$$S_N(r) = \frac{2\pi^{N/2} r^{N-1}}{\int_0^\infty e^{-t} t^{N/2-1} dt}, \tag{17}$$

and thus, Eq. (16) is written as

$$P_d = \frac{\int_0^T \frac{r^{N-1}}{2^{N/2-1}\sigma^N} \exp\left(-\frac{r^2}{2\sigma^2}\right) dr}{\int_0^\infty e^{-t} t^{N/2-1} dt}. \tag{18}$$

Letting $r = \sigma(2t)^{1/2}$ in the numerator of Eq. (18), one obtains

$$P_d = \frac{\int_0^{T^2/(2\sigma^2)} e^{-t} t^{N/2-1} dt}{\int_0^\infty e^{-t} t^{N/2-1} dt}. \tag{19}$$

By the lower incomplete gamma function, Eq. (19) is written as

$$P_d = \Gamma_p\left(\frac{N}{2}, \frac{T^2}{2\sigma^2}\right), \tag{20}$$

where $\Gamma_p(\cdot)$ represents the lower incomplete gamma function, i.e.,

$$\Gamma_p(a, x) = \frac{\int_0^x t^{a-1} e^{-t} dt}{\int_0^\infty e^{-t} t^{a-1} dt}. \tag{21}$$

By the inverse incomplete gamma function, T can also be written in terms of P_d , i.e.,

$$T = \sigma \sqrt{2\Gamma_{inv}\left(\frac{N}{2}, P_d\right)}. \tag{22}$$

So, for a specified P_d , T can be calculated by Eq. (22). Since the threshold is automatically calculated according to the detection rate, this algorithm has a larger applicability than the current methods based on range-profile matching.

Figure 1 shows the relation of T to P_d under different SNR_x 's. For the same SNR_x , when P_d increases, T increases. This also causes the false alarm rate to increase actually. Similarly, for the same P_d , when SNR_x increases, T decreases. This will cause the false alarm rate to decrease. The false alarm rate is the probability of misjudging a non-warhead target as a warhead. In practice, multiple range-profile matching can also be used to reduce the false alarm rate.

3.3 False alarm rate

For a radar recognition system, the false alarm rate is also an important parameter that must be discussed. Here, the false alarm rate is defined as the probability that a non-warhead target is misjudged as a warhead. When the SNR is very low, the threshold may be very high, and thus, the false alarm rate may be very high. In such a case, the algorithm is unreliable and cannot be used anymore.

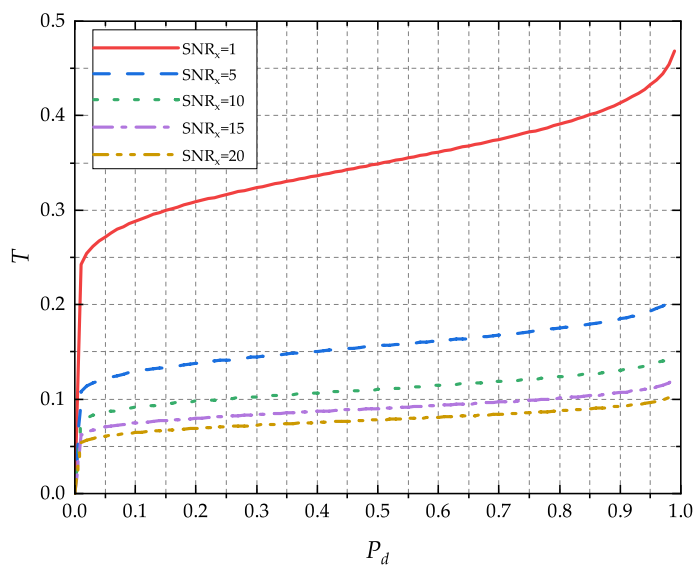


Fig. 1 Threshold versus detection rate under different SNR_x 's ($N=26$)

Assume that $x(n)$ and $s(n)$ are the range profiles of the non-warhead target and the warhead, respectively. They are limited to interval $1 \leq n \leq N$. The normalized correlation of $x(n)$ with $s(n)$ is defined as

$$R = \sum_{n=1}^N [\bar{x}(n)\bar{s}(n)], \quad (23)$$

where

$$\bar{x}(n) = \frac{x(n)}{\sqrt{\sum_{n=1}^N x^2(n)}}, \quad (24)$$

$$\bar{s}(n) = \frac{s(n)}{\sqrt{\sum_{n=1}^N s^2(n)}}. \quad (25)$$

$x(n)$ is considered to conform to the Rayleigh distribution, i.e., it has the probability density function

$$f_X(x) = \frac{x}{\sigma^2} e^{-\frac{x^2}{2\sigma^2}}, \quad x \geq 0. \quad (26)$$

This is derived from the assumption that the real part and the imaginary part of the complex range profile are independent Gaussian random variables with the mean 0 and the standard deviation σ [24]. It can be shown that the mean, the mean square, and the variance of $x(n)$ are, respectively,

$$E(X) = \sqrt{\frac{\pi}{2}}\sigma, \quad (27)$$

$$E(X^2) = 2\sigma^2, \quad (28)$$

$$V(X) = \frac{4 - \pi}{2}\sigma^2. \quad (29)$$

The norm of $x(n)$, ε , can be expressed as

$$\varepsilon = \sqrt{\sum_{n=1}^N x^2(n)} = \sqrt{N \cdot \frac{1}{N} \sum_{n=1}^N x^2(n)} = \sqrt{N \cdot E(X^2)} = \sigma\sqrt{2N}, \quad (30)$$

where $x(n)$ is assumed to be ergodic. So, the mean, the mean square, and the variance of $\bar{x}(n)$ are, respectively,

$$E(\bar{X}) = \frac{E(X)}{\varepsilon} = \frac{\sqrt{\frac{\pi}{2}}\sigma}{\sigma\sqrt{2N}} = \frac{1}{2}\sqrt{\frac{\pi}{N}}, \quad (31)$$

$$E(\bar{X}^2) = \frac{E(X^2)}{\varepsilon^2} = \frac{2\sigma^2}{(\sigma\sqrt{2N})^2} = \frac{1}{N}, \tag{32}$$

$$V(\bar{X}) = \frac{D(X)}{\varepsilon^2} = \frac{\frac{4-\pi}{2}\sigma^2}{(\sigma\sqrt{2N})^2} = \frac{1}{N}\left(1 - \frac{\pi}{4}\right). \tag{33}$$

Similarly, it can be shown that the mean, the mean square, and the variance of $\bar{s}(n)$ are, respectively,

$$E(\bar{S}) = \frac{1}{2}\sqrt{\frac{\pi}{N}}, \tag{34}$$

$$E(\bar{S}^2) = \frac{1}{N}, \tag{35}$$

$$V(\bar{S}) = \frac{1}{N}\left(1 - \frac{\pi}{4}\right). \tag{36}$$

Assume that $x(n)$ and $s(n)$ are independent. Then, the mean, the mean square, and the variance of $\bar{x}(n)\bar{s}(n)$ are, respectively,

$$E(\bar{X}\bar{S}) = E(\bar{X})E(\bar{S}) = \frac{\pi}{4N}, \tag{37}$$

$$E(\bar{X}^2\bar{S}^2) = E(\bar{X}^2)E(\bar{S}^2) = \frac{1}{N^2}, \tag{38}$$

$$V(\bar{X}\bar{S}) = E(\bar{X}^2\bar{S}^2) - [E(\bar{X}\bar{S})]^2 = \frac{1}{N^2}\left(1 - \frac{\pi^2}{16}\right). \tag{39}$$

According to the central limit theorem, roughly, R conforms to the Gaussian distribution and has the probability density function

$$f(R) = \frac{1}{\sqrt{2\pi}\sigma_R} \exp\left(-\frac{(R - \mu_R)^2}{2\sigma_R^2}\right), \tag{40}$$

where

$$\mu_R = E(R) = N \cdot E(\bar{X}\bar{S}) = \frac{\pi}{4}, \tag{41}$$

$$\sigma_R = V(R) = N \cdot V(\bar{X}\bar{S}) = \frac{1}{N}\left(1 - \frac{\pi^2}{16}\right). \tag{42}$$

In our algorithm, the false alarm rate is the probability of $D \leq T$ for a non-warhead target. Substituting Eq. (5) into this inequality, we obtain $R \geq 1 - T^2/2$. Thus, the false alarm rate is also the probability of $R \geq 1 - T^2/2$ for a non-warhead target, i.e.,

$$P_{fa} = \int_{1-\frac{T^2}{2}}^{\infty} f(R) dR. \quad (43)$$

Equation (43), along with Eqs. (40), (41), and (42), can be used to calculate the false alarm rate and determine the reliability of the algorithm although they are derived based on some assumptions. The algorithm is considered to be unreliable and cannot be used anymore when the false alarm rate is high enough.

4 Simulation results and analyses

Simulated range profiles are used to test our algorithm. The data obtained through computer simulation have practical significance as well. Many radar systems for ballistic missile defense operate in the X-band, i.e., the central frequency is 8-12 GHz. So, we choose 10 GHz as the central frequency in the simulation. The bandwidth determines the range resolution of the radar. The range resolution of the radar is $c/(2B)$ [16], where c is the speed of the light, and B is the bandwidth. We choose a bandwidth of 1 GHz and the corresponding range resolution is about 0.15 meter, which can well show the structural characteristics of a typical warhead. The frequency interval determines the length of the range profile. The length of the range profile is $c/(2\Delta)$, where Δ is the frequency interval. We choose the frequency interval as 5 MHz, and the corresponding length of the range profile is 30 m.

The range profile of a target is simulated in two steps [25]. In the first step, a software for electromagnetic calculation, the CST Microwave Studio [26], is used to simulate the frequency response of the target. The VV polarization is adopted, and 201 frequencies, from 9.5 to 10.5 GHz with a 5 MHz interval, are chosen. In the second step, the range profile is calculated from the frequency response. First, the frequency response is multiplied by a Hamming window, shifted to the baseband, extended with a 256-point period, and limited to the indexes from 0 to 255. Then, the resulting sequence is used to find the range profile by the inverse fast Fourier transform (IFFT) [27] and a 128-point circular shift.

4.1 Dataset

A dataset, which consists of the range profiles from a warhead in typical illumination directions, is built to test our algorithm.

The shape of the simulated warhead is shown in Fig. 2. In practice, a warhead is generally cone-like [28–30]. The radius of the cone bottom d is 0.25 m. The height of the cone h is 1.5 m. The radius of the spherical crown ρ is 0.05 m. The coordinate system is selected so that the origin is situated at the centroid of the cone, and the z -axis is directed up the axis of the cone. Thus, the distance between the xy -plane and the cone bottom l is 0.375 m. M is the top of the warhead. P and Q are the intersections between the bottom circle of the warhead and the plane determined by the axis of the warhead and the line of sight (LOS) of the radar. Assumed that the surface of the warhead has a perfect electric conductivity.

Ballistic missile defense systems generally provide the defense against incoming warheads. In this case, γ , the angle between the axis of the warhead and the LOS of the radar is an acute angle. In practice, γ is generally between 10° to 70° . Thus, we set γ from 10° to

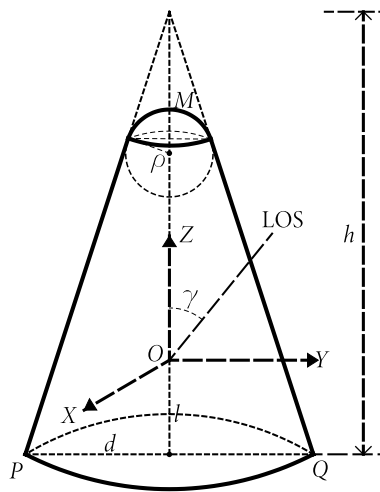


Fig. 2 The structure of the warhead target

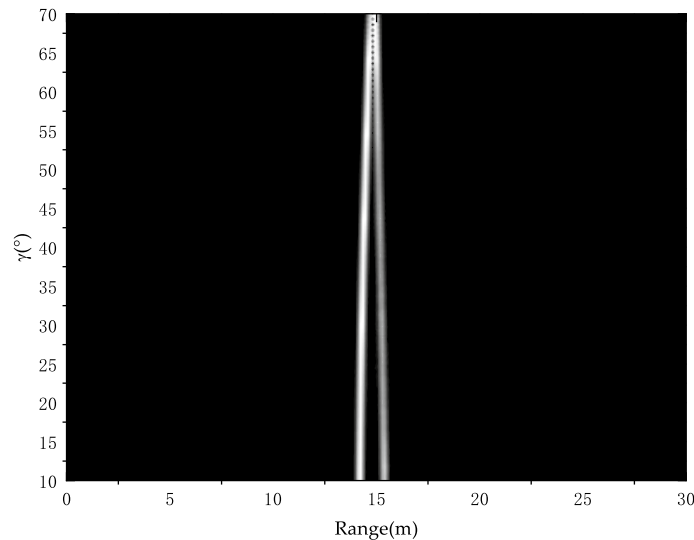


Fig. 3 Range profiles of warhead at different angles

70° to reduce the pressure of the range-profile matching. Since the range profile is very sensitive to γ [31], the increment of γ is set to 0.1°.

Figure 3 shows the range profiles in the dataset. We can see that in typical illumination directions, the range profile of the warhead has two peaks. This is a significant feature of the range profile. Theoretically, the two peaks result from two strong scatters on the warhead, M and Q , and the distance between the two peaks is close to the projection of MQ on the LOS of the radar.

4.2 Recognition of Warhead

The range profile of the warhead with $\gamma = 30^\circ$ and $SNR_x=5$ is used to test our algorithm. In all the simulations, the white Gaussian noise is used. The detection rate P_d is set to 0.9, and the threshold T is thus found to be 0.16694. Due to the noise, the most similar

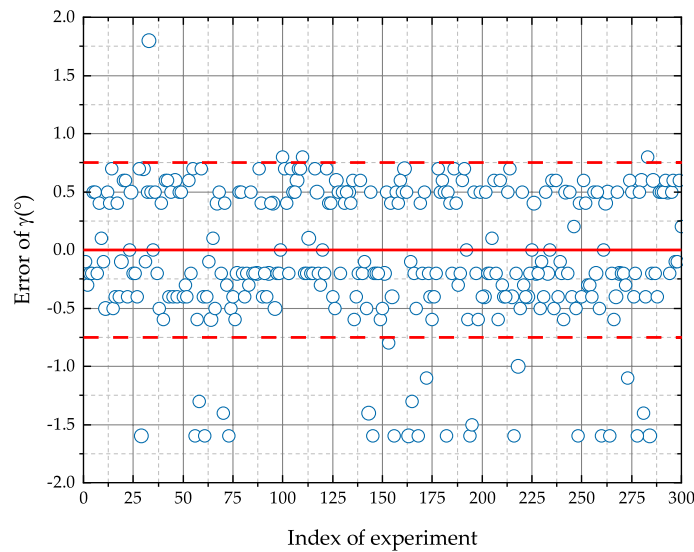


Fig. 4 Error of γ in different experiments

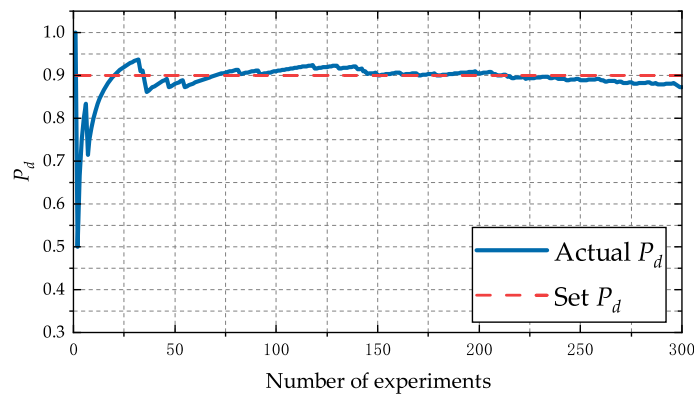


Fig. 5 Detection rate versus number of experiments

range profile is found to be the range profile with $\gamma = 29.6^\circ$. The target is regarded as a warhead because D , the deviation of its range profile from the most similar range profile, is 0.1137, less than the threshold T . In addition, according to the discussion in Sect. 3.3, the false alarm rate is 1.5768×10^{-42} , a very low level. It can be seen that the proposed algorithm can recognize the warhead target correctly.

More experiments are carried out with the same γ and SNR_x but different noises. The detection rate P_d is still set to 0.9. Figure 4 shows the difference between the γ of the most similar range profile and the true γ in 300 experiments. From the figure, one can see that most errors fall between $\pm 0.75^\circ$. Figure 5 depicts the variation of P_d with the number of experiments, from which one can see that as the number of experiments increases, P_d tends to be stable and close to the preset detection rate 0.9.

More experiments are also carried out with the same γ , $\text{SNR}_x=10$ and different noises. The detection rate P_d is still set to 0.9. Figure 6 shows the difference between the γ of the most similar range profile and the true γ in different experiments. Note

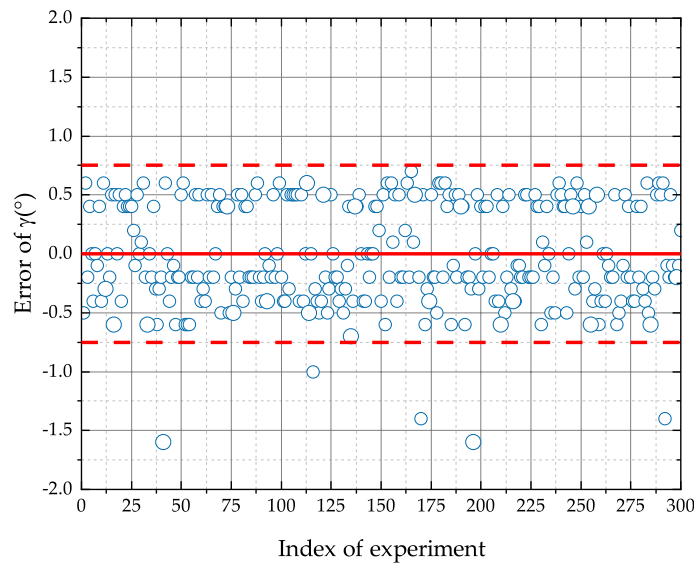


Fig. 6 Error of γ in different experiments when $SNR_x=10$

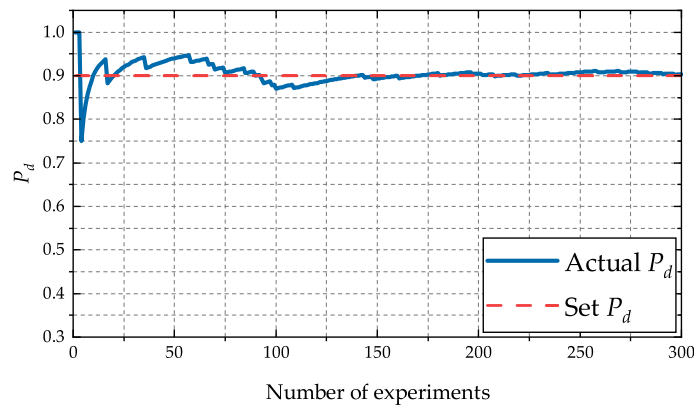


Fig. 7 Detection rate versus number of experiments when $SNR_x=10$

that when SNR_x increases, the error of γ is more centralized around 0. Figure 7 shows the variation of P_d with the number of experiments. We can see that P_d still tends to be stable and close to the preset detection rate 0.9 as the number of experiments increases.

We also use the range profiles of the warhead with other γ 's to test the proposed algorithm. In this experiment, the range profile of the warhead with $\gamma = 45^\circ$ and $SNR_x=5$ is used. Similarly, the detection rate P_d is set to 0.9, and the threshold T is thus found to be 0.16694. Due to the noise, the most similar range profile is found to be the range profile with $\gamma = 45.2^\circ$. The target is correctly regarded as a warhead because D , the deviation of its range profile from the most similar range profile, is 0.1152, less than the threshold T . Figures 8 and 9 show the error of γ and the variation of P_d in 300 experiments, respectively, and similar results are obtained.

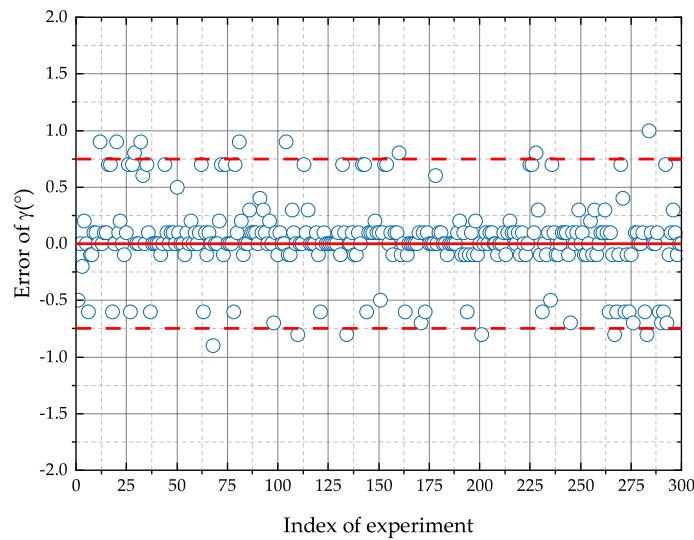


Fig. 8 Error of γ in different experiments when $SNR_x=5$ and $\gamma = 45^\circ$

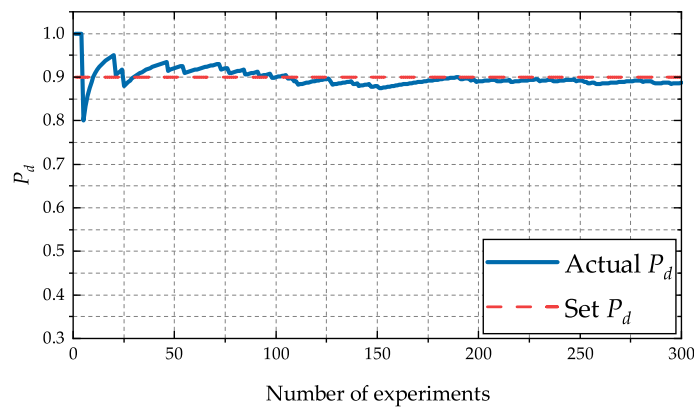


Fig. 9 Detection rate versus number of experiments when $SNR_x=5$ and $\gamma = 45^\circ$

4.3 Recognition of typical decoys

In the following experiments, the noise is added such that $SNR_x=5$. The detection rate P_d is set to 0.9, and so, the threshold T is found to be 0.16694.

The range profile of a sphere is used to test the proposed algorithm (Fig. 10). The sphere has a radius of 0.25 m, and its surface is assumed to have a perfect electric conductivity. Its structure is very simple, and so, we do not show its structure model here.

Each range profile in the dataset is compared with the range profile of the sphere target to find the most similar range profile. The most similar range profile is found to be the range profile with $\gamma = 69.7^\circ$. The target is not classified as a warhead because D , the deviation of its range profile from the most similar range profile, is found to be 0.42289, larger than the threshold T .

The range profile of a fragment with $\gamma = 10^\circ$ and $\theta = 20^\circ$ (θ is the angle between the projection of the LOS on the xy -plane and the x -axis) is also used to test our algorithm. Figure 11 shows the range profile of the fragment in the simulation. Figure 12 shows the fragment illuminated by the radar, where the inner radius r' is 0.25 m, the outer radius

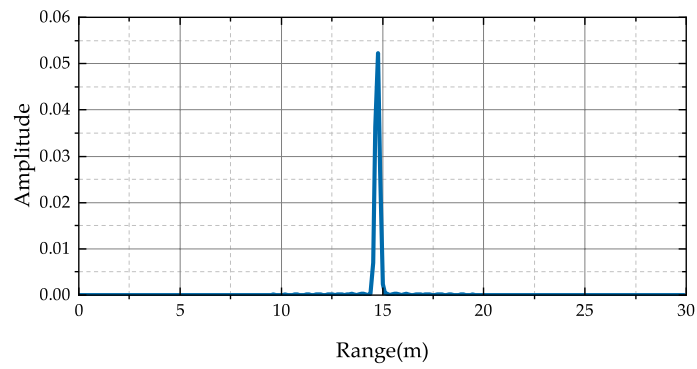


Fig. 10 Range profile of a sphere

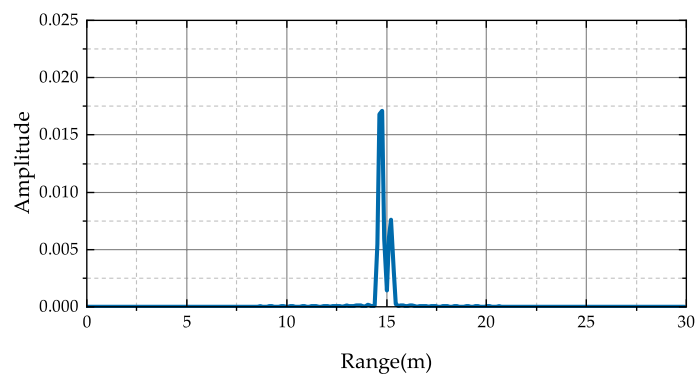


Fig. 11 The range profile of the fragment model ($\gamma = 10^\circ$ and $\theta = 20^\circ$)

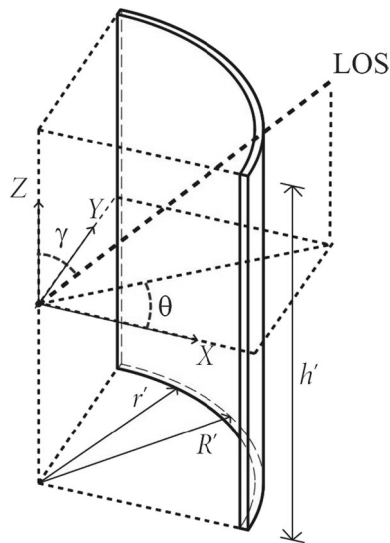


Fig. 12 The structure of the fragment model

R' is 0.26 m, and the height h' is 0.5 m. Assume that its surface has a perfect electric conductivity.

The most similar range profile is found to be the range profile with $\gamma = 54.3^\circ$. The target is not classified as a warhead because D , the deviation of its range profile from the most similar range profile, is found to be 0.22453, larger than the threshold T .

Furthermore, we also use the range profiles of the fragment with other γ 's and θ 's to test our algorithm and obtain similar results.

In order to test the effectiveness of the deviation in recognizing warheads from decoys, 300 experiments are carried out for the warhead ($\gamma = 30^\circ$), the sphere, and the fragment ($\gamma = 10^\circ$ and $\theta = 20^\circ$), respectively. SNR_x is set as 5 in all experiments. Figure 13 shows the deviation of each target in each experiment.

As we see, the deviation of the warhead is almost always less than the threshold, but the deviation of the sphere and the deviation of the fragment are always larger than the threshold. This indicates that our algorithm is effective in recognizing warheads from simple decoys, like spheres and fragments. This algorithm, however, cannot be used to exclude high-imitation decoys from warheads because high-imitation decoys have similar range profiles to warheads. More features, like micro-motion features, have to be considered in such cases.

The computational efficiency of this algorithm is an important factor in practical applications. The program is written in MATLAB on a Dell OptiPlex 5080 (2.9-GHz

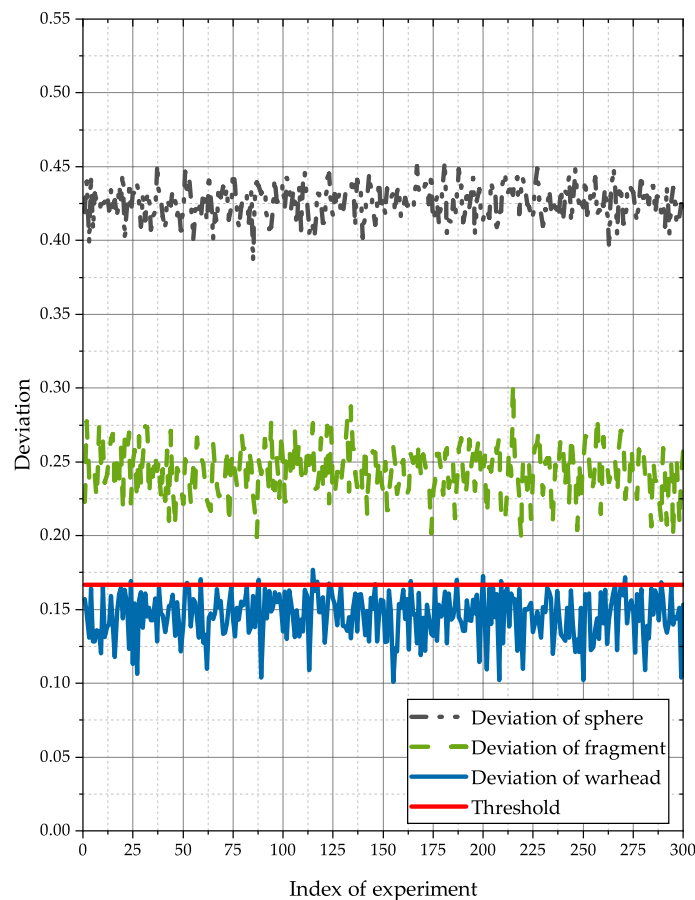


Fig. 13 Deviations of different targets

Core i7-10700 CPU, 16-GB RAM), and no parallel processing is used. Typically, the time of the entire algorithm is about 10 milliseconds. Usually, this time is less than a pulse repetition period, which means that this algorithm is suitable for real-time applications. The computation time increases linearly with the size of the dataset. When the size of the dataset is very large, parallel processing can be used to reduce the computation time. The whole dataset is divided into different subsets. The range profile of interest is compared to the range profiles in different subsets at the same time. The comparison results with different subsets are compared to find the best matched range profile in the whole dataset.

4.4 Comparison with traditional method

In the traditional matching-recognition method, the recognition threshold is selected empirically and fixed, and the detection rate changes with the SNR. Figure 14 shows the variation of the detection rate with the SNR in the traditional method. Here, the recognition threshold is selected as 0.14, and 100 experiments are carried out under each SNR. It can be seen that in the case of low SNRs, the detection rate of the traditional method is low. This limits its application because the detection rate of a method should be higher enough to be useful. Figure 14 also shows the variation of the detection rate with the SNR in the proposed method. Here, the recognition threshold is selected such that the detection rate is a constant 0.9, and 100 experiments are carried out under each SNR. It can be seen that the actual detection rate is always around the preset detection rate, even for low SNRs. Evidently, the proposed method has a larger applicability than the traditional method.

5 Conclusions

The proposed algorithm is effective for warhead recognition in the defense of ballistic missiles. The range profiles from the warheads of interest in typical illumination directions form a dataset. Each range profile in the dataset is compared to the range profile of the target under observation, and the most similar range profile is found. The target is considered as a warhead if the deviation of its range profile from the most similar range

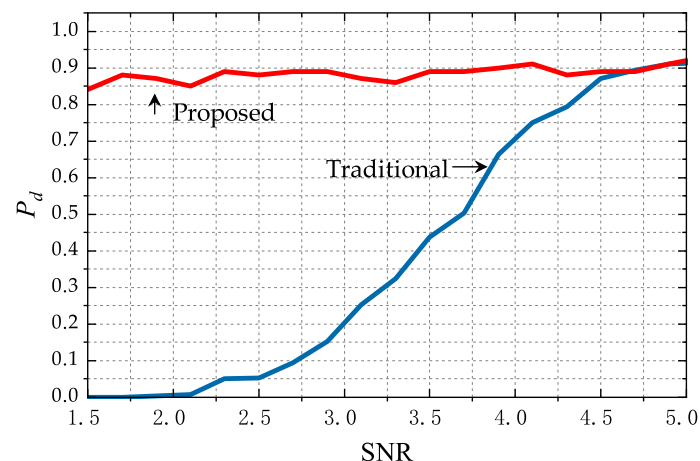


Fig. 14 Detection rate versus SNR for traditional and proposed methods

profile is less than or equal to a threshold. The threshold is chosen such that the detection rate is constant. Since the threshold is automatically calculated according to the detection rate, this algorithm has a larger applicability than the current methods based on range profile recognition. The results of computer-simulated data indicate the effectiveness of this algorithm.

This algorithm can be used to exclude simple decoys, such as spheres and fragments, from warheads because simple decoys have different range profiles from warheads. It cannot be used to exclude high-imitation decoys from warheads because high-imitation decoys have similar range profiles to warheads. In such a situation, more features, like micro-motion features, have to be considered.

Acknowledgements

The authors would like to express their sincere thanks to the editors and anonymous reviewers.

Author Contributions

This study was designed by DT and supervised by JW. DT created the software of this study and collected the data. Data analysis was performed by DT and JW. DT and JW prepared the manuscript. Both authors critically revised, read and approved the final manuscript.

Funding

This work is supported by the National Natural Science Foundation of China, Grant Number U2031127 and the Shanghai Academy of Spaceflight Technology Foundation.

Availability of data and materials

Not applicable.

Declarations

Ethics approval and consent to participate

Not applicable.

Consent for publication

Not applicable.

Competing interests

The authors declare that they have no competing interests. The funders had no role in the design of the study; in the collection, analyses, or interpretation of data; in the writing of the manuscript; or in the decision to publish the results.

Received: 18 December 2023 Accepted: 17 February 2024

Published online: 28 February 2024

References

1. J.-Y. Lee, B.-U. Jo, G.-H. Moon, M.-J. Tahk, J. Ahn, Intercept point prediction of ballistic missile defense using neural network learning. *Int. J. Aeronaut. Space Sci.* **21**, 1092–1104 (2020)
2. B.M. Wade, A multi-objective optimization of ballistic and cruise missile fire plans based on damage calculations from missile impacts on an airfield defended by an air defense artillery network. *J. Defense Model. Simul.* **16**(2), 103–107 (2019)
3. W.W. Camp, J.T. Mayhan, R.M. O'Donnell, Wideband radar for ballistic missile defense and range-doppler imaging of satellites. *Lincoln Lab J.* **12**(2), 267–280 (2000)
4. X. Li, V. Jilkov, Survey of maneuvering target tracking. part ii: Motion models of ballistic and space targets. *IEEE Trans. Aerosp. Electron. Syst.* **46**(1), 96–119 (2010)
5. Z.W. Zhang, Y.S. Liu, Y.H. Wang, X.Y. Fan, Development Overview of Russian Ballistic Missile and Missile Defense System. Paper presented at the SPIE International Conference on Mechanical Design and Simulation, Wuhan, China, 18–20 Mar. 2022 (2022)
6. M.M.H. Amir, S. Maresca, G. Serafino, P. Ghelfi, A. Bogoni, Target RCS Modeling and CFAR Detection Performance with Photonics-based Distributed Multi-Band MIMO Radars. Paper presented at the 21st International Radar Symposium (IRS), Berlin, Germany, 21–22 Jun. 2021. (2021)
7. V.C. Chen, S.-S. Ho, H. Wechsler, Micro-doppler effect in radar: phenomenon, model and simulation study. *IEEE Trans. Aerosp. Electron. Syst.* **42**(1), 2–21 (2006)
8. V.C. Chen, Radar detection of multiple moving targets in clutter using time-frequency radon transform. Paper presented at the 14th Conference on Signal and Data Processing of Small Targets, Orlando, FL, 02–04 Apr., 2002 (2002)
9. W. Yu, J. Wang, Phase Adjustment for Extraction of Micro-Motion Information of Ballistic Targets. Paper presented at the International Congress on Image and Signal Processing, Chongqing, China, 16–18 Oct. 2012. (2012)

10. B. Tian, Z.J. Lu, Y.X. Liu, X. Li, Review on interferometric isar 3d imaging: concept, technology and experiment. *Signal Process.* **153**, 164–187 (2018)
11. H. Deng, Radar Target Recognition Based on Orthogonal Range Profile Extraction. Paper presented at the IEEE Antennas and Propagation Society International Symposium. Columbus, OH, USA, 22–27 June 2003. (2003)
12. J.W. Hyde, C.M. Alabaster, Correlation of Target Transfer Functions and Range Profiles as a Function of Aspect Angle and Resolution. Paper presented at IET Waveform Diversity and Digital Radar Conference, London, UK, 8 Dec. 2008. (2008)
13. B. Xie, J.F. Wang, Recognition of Warhead in Ballistic Missile Defense. Paper presented at International Congress on Image and Signal Processing, Dalian, China, 14–16 Oct. 2014. (2014)
14. M. Skolnik, G. Linde, K. Meads, Senrad: an advanced wideband air-surveillance radar. *IEEE Trans. Aerosp. Electron. Syst.* **37**, 1163–1175 (2001)
15. W. Chao, G. Cuiling, S. Wanjie, W. Shunjun, Research on Real Time Range Profile of Marine Targets and Its Characteristics. Paper presented at 1st Asian and Pacific Conference on Synthetic Aperture Radar, Huangshan, China, 5–9 Nov. 2007. (2007)
16. B. Zheng, X. Mengdao, W. Tong, *Radar Profiling Technique* (Electronic Industry Publishing House, Beijing, 2005)
17. J. Sun, Modern Pattern Recognition, pp. 14–19. National University of Defense Technology Press, Changsha, China (2002)
18. S. Luo, S. Li, A Novel Approach of Automatic Target Recognition Using High Resolution Radar Range Profiles. Paper presented at International Symposium on Microwave, Antenna, Propagation and EMC Technologies for Wireless Communications, Hangzhou, China, 14–17 Aug. 2007. (2007)
19. L. Savy, C. Gaie, Model-Based Classification of Aircraft Range Profiles Using Data Association Algorithms. Paper presented at IEEE Radar Conference, Waltham, MA, USA, 17–20 Apr. 2007. (2007)
20. D.L. Tan, J.F. Wang, Recognition of Warhead by Range-Profile Matching. Paper presented at IEEE IGARSS, Brussels, Belgium, 11–16 July 2021. (2021)
21. K. Zebiri, A. Mezache, Radar cfar detection for multiple-targets situation for weibull and log-normal distributed clutter. *SIVIP* **15**, 1671–1678 (2021)
22. V.M. Artyushenko, V.I. Volovach, Identification of the distribution parameters of additive and multiplicative non-gaussian noise. *Optoelectron. Instrum. Data Process.* **53**, 230–236 (2017)
23. E.J. Valentine, A metric characterization of "spherical" surfaces in n-dimensional hyperbolic space. *Journal für die reine und angewandte Mathematik.* **251**, 142–152 (1971)
24. O. Chris, S. Quegan, *Understanding Synthetic Aperture Radar Images* (SciTech Publishing, Chennai, 2004)
25. W.T. Lv, J.F. Wang, W.X. Yu, Simulation of echoes from ballistic targets. *IEEE Antennas Wirel. Propag. Lett.* **13**, 1361–1364 (2014)
26. CST Suite 2013: CST AG. CST, Darmstadt, Germany (2013)
27. A.V. Oppenheim, R.W. Schaffer, *Discrete-Time Signal Processing*, 3rd edn. (Publishing House of Electronics Industry, Beijing, 2019)
28. D. Feng, L. Xu, D. Dai, Radar Target Recognition Method Based on Physical-Statistical Model. Paper presented at IEEE International Conference on Signal Processing, Communication and Computing, Hong Kong, China, 12–15 Aug. 2012. (2012)
29. G. Martynenko, M. Chernobryvko, K. Avramov, V. Martynenko, A. Tonkonozhenko, V. Kozharin, D. Klymenko, Numerical simulation of missile warhead operation. *Adv. Eng. Softw.* **123**, 93–103 (2018)
30. V.M. Gold, Fragmentation model for large l/d (length over diameter) explosive fragmentation warheads. *Defence Technol.* **13**(4), 300–309 (2017)
31. H. Wu, G. Li, J. Zhou, High-resolution Range Profiles Recognition Based on SAR/ISAR Images. Paper presented at IEEE 3rd Advanced Information Management, Communicates, Electronic and Automation Control Conference (IMCEC), Chongqing, China, 11–13 Oct. 2019. (2019)

Publisher's Note

Springer Nature remains neutral with regard to jurisdictional claims in published maps and institutional affiliations.